International Journal of Engineering & Applied Sciences (IJEAS)
Vol.11, Issue 2 (2019) 387-400
http://dx.doi.org/10.24107/ijeas.569798
Int J Eng Appl Sci 11(2) (2019) 387-400

Finite Element Model of Functionally Graded Nanobeam for Free Vibration Analysis

Büşra Uzun [a], Mustafa Özgür Yaylı [b]*

[a,b] Bursa Uludag University, Civil Engineering Department
Division of Mechanics, Bursa-TURKIYE

[*]E-mail address: buzun@uludag.edu.tr [a*], ozguryayli@uludag.edu.tr [b]

ORCID numbers of authors:
0000-0002-7636-7170[a], 0000-0003-2231-170X[b]*

Received date: 24.05.2019
Accepted date: 12.06.2019

Abstract

In the present study, free vibration of functionally graded (FG) nanobeam is investigated. The variation of material properties is assumed in the thickness direction according to the power law. FG nanobeam is modeled as Euler-Bernoulli beam with different boundary conditions and investigated based on Eringen's nonlocal elasticity theory. Governing equations are derived via Hamilton principle. Frequency values are found by using finite element method. FG nanobeam is composed of silicon carbide (SiC) and stainless steel (SUS304). The effects of dimensionless small-scale parameters (e_0a/L), power law exponent (k) and boundary conditions on frequencies are examined for FG nanobeam.

Keywords: Functionally graded nanobeam, nonlocal elasticity theory, free vibration, finite element method

1. Introduction

Functionally graded materials (FGMs) are defined as special composites which material properties change continuously along with direction of the material. FGMs are mostly composed of ceramic and metal. Thus the ceramic can resist high temperature in thermal environments, while the metal can reduce the stress occurring on the ceramic surface at the earlier case of cooling. FGMs are utilized in various applications such as aviation, mechanical, electronics, nuclear, optics, chemical, biomedicine and civil engineering [1-2].

The classical continuum theories lose their validity when the dimensions are reduced because they lack internal/additional material small-scale parameters. For this reason, some researchers have been used some higher order theories that take into account small-scale effect analysis of micro and nano structures [3-5]. Among higher order theories, nonlocal elasticity theory [6] have been widely studied recently [7-21]. Ebrahimi et al. [2] presented the applicability of differential transformation method (DTM) in investigations on vibrational characteristics of FG size-dependent nanobeams. Civalek and Demir [22] developed elastic beam model using nonlocal elasticity theory and Euler–Bernoulli beam theory for the bending analysis of microtubules (MTs). Kadıoğlu and Yaylı [23] studied buckling analysis of a nano sized beam by using Timoshenko beam theory and Eringen's nonlocal elasticity theory. Zargaripoor et al. [24] investigated free vibration of functionally graded nanoplate by using Eringen's nonlocal theory.

In this study, vibration characteristics of FG nanobeams are investigated. The variation of material properties is assumed in the thickness direction based on the power law. FG nanobeam is composed of silicon carbide (SiC) and stainless steel (SUS304). Governing equations are derived via Hamilton principle. The vibration behaviours of SiC/SUS304 FG nanobeam with simply-supported (S-S) and clamped-clamped (C-C) boundary conditions are analyzed using nonlocal finite element formulation. The effects of small-scale parameters (e_0a/L), power law exponents (k) and boundary conditions on frequencies are examined for FG nanobeam.

2. Functionally Graded Euler-Bernoulli Beam

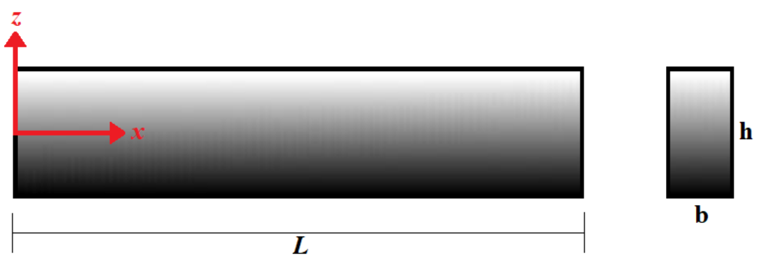

Fig. 1. Ilustration of FG beam

L, b and h are length, width and thickness of the FG beam, respectively. The material properties of the beam are assumed to vary continuously in the thickness direction. The effective material property of FG beam is expressed by the power law as follows [9]

$$P(z) = (P_U - P_L)\left(\frac{z}{h} + \frac{1}{2}\right)^k + P_L \tag{1}$$

Here $P(z)$ is the effective material property of the beam, P_U and P_L are the material property at the upper and lower surfaces of the beam, k is the power law exponent (non-negative variable parameter). $P(z)$ indicates to the properties of the beam components such as the elastic module (E), density (ρ) etc. and can be transformed into the following forms

$$E(z) = (E_U - E_L)\left(\frac{z}{h} + \frac{1}{2}\right)^k + E_L \tag{2}$$

$$\rho(z)=(\rho_U-\rho_L)\left(\frac{z}{h}+\frac{1}{2}\right)^k+\rho_L \tag{3}$$

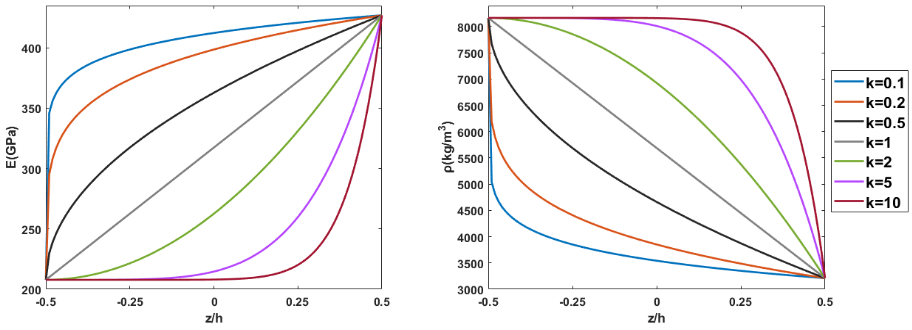

Fig. 2. The variation of material properties through the thickness direction

The displacements for Euler-Bernoulli beam can be written as follows [13]

$$u_1(x,z,t)=u(x,t)-z\frac{\partial w(x,t)}{\partial x} \tag{4a}$$

$$u_2(x,z,t)=0 \tag{4b}$$

$$u_3(x,z,t)=w(x,t) \tag{4c}$$

Here u_1, u_2 and u_3 are the displacements in the x, y, z directions, respectively. u and w denote longitudinal and transverse displacements of any point on the neutral axis, respectively. Strains of the Euler-Bernoulli beam as follows

$$\varepsilon_{xx}=\frac{\partial u(x,t)}{\partial x}-z\frac{\partial^2 w(x,t)}{\partial x^2},\ \varepsilon_{xy}=\varepsilon_{yx}=\varepsilon_{xz}=\varepsilon_{zx}=\varepsilon_{yy}=\varepsilon_{yz}=\varepsilon_{zy}=\varepsilon_{zz}=0 \tag{5}$$

ε_{xx} is the non-zero only strain component. Stress, normal force and moment expressions for the functionally graded beam are written as follows

$$\sigma_{xx}=E(z)\varepsilon_{xx} \tag{6}$$

$$N=A_1\frac{\partial u}{\partial x}-B_1\frac{\partial^2 w}{\partial x^2},\ M=B_1\frac{\partial u}{\partial x}-D_1\frac{\partial^2 w}{\partial x^2} \tag{7}$$

A_1, B_1 ve D_1 are expressed as

$$A_1 = \int_A E(z)dA,\ B_1 = \int_A E(z)zdA,\ D_1 = \int_A E(z)z^2 dA \tag{8}$$

The Hamilton principle to be used to obtain equations of motion is expressed as follows [25]

$$\int_0^T (\delta S - \delta T)dt = 0 \tag{9}$$

Where *S* and *T* are the strain energy and kinetic energy, respectively. *S* and *T* for an element which has volume *V* and length *L* is as below

$$S = \frac{1}{2}\int_V \sigma_{xx}\varepsilon_{xx} dV \tag{10}$$

$$T = \frac{1}{2}\int_V \rho(z)\left(\left(\frac{\partial u_1}{\partial t}\right)^2 + \left(\frac{\partial u_2}{\partial t}\right)^2 + \left(\frac{\partial u_3}{\partial t}\right)^2\right)dV \tag{11}$$

The first variation of the strain and kinetic energy are obtained as follows

$$\begin{aligned}\delta\int_0^T Sdt &= \int_0^T\int_0^L \left(N\delta\left(\frac{\partial u}{\partial x}\right) - M\delta\left(\frac{\partial^2 w}{\partial x^2}\right)\right)dxdt \\ &= \int_0^T\int_0^L \left(\left(A_1\frac{\partial u}{\partial x} - B_1\frac{\partial^2 w}{\partial x^2}\right)\delta\left(\frac{\partial u}{\partial x}\right) - \left(B_1\frac{\partial u}{\partial x} - D_1\frac{\partial^2 w}{\partial x^2}\right)\delta\left(\frac{\partial^2 w}{\partial x^2}\right)\right)dxdt\end{aligned} \tag{12}$$

$$\delta\int_0^T Tdt = \int_0^T\int_0^L \left(I_0\left(\frac{\partial u}{\partial t}\delta\left(\frac{\partial u}{\partial t}\right) + \frac{\partial w}{\partial t}\delta\left(\frac{\partial w}{\partial t}\right)\right) - I_1\left(\frac{\partial u}{\partial t}\delta\left(\frac{\partial^2 w}{\partial x\partial t}\right) + \frac{\partial^2 w}{\partial x\partial t}\delta\left(\frac{\partial u}{\partial t}\right)\right) + I_2\frac{\partial^2 w}{\partial x\partial t}\delta\left(\frac{\partial^2 w}{\partial x\partial t}\right)\right)dxdt \tag{13}$$

Here I_0, I_1 and I_2 are expressed as

$$I_0 = \int_A \rho(z)dA,\ I_1 = \int_A \rho(z)zdA,\ I_2 = \int_A \rho(z)z^2 dA \tag{14}$$

Substituting Equations (12) and (13) into Equation (9), we obtain the equilibrium equations from the Euler-Lagrange equation as follows

$$\delta u : \frac{\partial N}{\partial x} = I_0 \frac{\partial^2 u}{\partial t^2} - I_1 \frac{\partial^3 w}{\partial x \partial t^2} \tag{15}$$

$$\delta w : \frac{\partial^2 M}{\partial x^2} = I_0 \frac{\partial^2 w}{\partial t^2} + I_1 \frac{\partial^3 u}{\partial x \partial t^2} - I_2 \frac{\partial^4 w}{\partial x^2 \partial t^2} \tag{16}$$

3. Nonlocal Functionally Graded Nanobeam

The nonlocal constitutive formulation is [6]

$$\left[1 - \left(e_0 a\right)^2 \nabla^2\right] \sigma_{ij} = C_{ijkl} \varepsilon_{kl} \tag{17}$$

Where σ_{ij} is the stress tensor, C_{ijkl} is the fourth-order elastic module tensor, ε_{kl} is the strain tensor, e_0 is a material constant which is determined experimentally, a is the internal characteristic length. For Euler–Bernoulli FG nanobeam, Equation (17) can be rewritten as

$$\sigma_{xx} - \left(e_0 a\right)^2 \frac{\partial^2 \sigma_{xx}}{\partial x^2} = E(z) \varepsilon_{xx} \tag{18}$$

Integrating Equation (18) over the cross-section area, we obtain the axial force-strain relation as

$$N - (e_0 a)^2 \frac{\partial^2 N}{\partial x^2} = A_1 \frac{\partial u}{\partial x} - B_1 \frac{\partial^2 w}{\partial x^2} \tag{19}$$

Multiplying Equation (18) by z and integrating over the cross-section area, we get the moment-curvature relation as

$$M-(e_0a)^2\frac{\partial^2 M}{\partial x^2}=B_1\frac{\partial u}{\partial x}-D_1\frac{\partial^2 w}{\partial x^2} \tag{20}$$

Differentiating Equation (15) with respect to x, then substituting Equation (19) we obtain Equation (21). And substituting Equation (16), we obtain Equation (22).

$$N=A_1\frac{\partial u}{\partial x}-B_1\frac{\partial^2 w}{\partial x^2}+(e_0a)^2\left(I_0\frac{\partial^3 u}{\partial x\partial t^2}-I_1\frac{\partial^4 w}{\partial x^2\partial t^2}\right) \tag{21}$$

$$M=B_1\frac{\partial u}{\partial x}-D_1\frac{\partial^2 w}{\partial x^2}+(e_0a)^2\left(I_0\frac{\partial^2 w}{\partial t^2}+I_1\frac{\partial^3 u}{\partial x\partial t^2}-I_2\frac{\partial^4 w}{\partial x^2\partial t^2}\right) \tag{22}$$

4. Finite Element Formulation

The variational statement of FG Euler–Bernoulli nanobeam has the following form

$$\int_0^T\int_0^L\left(\begin{array}{l}\left(A_1\frac{\partial u}{\partial x}\delta\left(\frac{\partial u}{\partial x}\right)-B_1\frac{\partial^2 w}{\partial x^2}\delta\left(\frac{\partial u}{\partial x}\right)+(e_0a)^2\left(I_0\frac{\partial^3 u}{\partial x\partial t^2}\delta\left(\frac{\partial u}{\partial x}\right)-I_1\frac{\partial^4 w}{\partial x^2\partial t^2}\delta\left(\frac{\partial u}{\partial x}\right)\right)\right)\\ -\left(\begin{array}{l}B_1\frac{\partial u}{\partial x}\delta\left(\frac{\partial^2 w}{\partial x^2}\right)-D_1\frac{\partial^2 w}{\partial x^2}\delta\left(\frac{\partial^2 w}{\partial x^2}\right)\\ +(e_0a)^2\left(I_0\frac{\partial^2 w}{\partial t^2}\delta\left(\frac{\partial^2 w}{\partial x^2}\right)+I_1\frac{\partial^3 u}{\partial x\partial t^2}\delta\left(\frac{\partial^2 w}{\partial x^2}\right)-I_2\frac{\partial^4 w}{\partial x^2\partial t^2}\delta\left(\frac{\partial^2 w}{\partial x^2}\right)\right)\end{array}\right)\\ -\left(I_0\left(\frac{\partial u}{\partial t}\delta\left(\frac{\partial u}{\partial t}\right)+\frac{\partial w}{\partial t}\delta\left(\frac{\partial w}{\partial t}\right)\right)-I_1\left(\frac{\partial u}{\partial t}\delta\left(\frac{\partial^2 w}{\partial x\partial t}\right)+\frac{\partial^2 w}{\partial x\partial t}\delta\left(\frac{\partial u}{\partial t}\right)\right)+I_2\frac{\partial^2 w}{\partial x\partial t}\delta\left(\frac{\partial^2 w}{\partial x\partial t}\right)\right)\end{array}\right)dxdt \tag{23}$$

ϕu and ϕw are the interpolation shape functions and they are expressed as below

$$[\phi_u]=\left[1-\frac{x}{L}\quad \frac{x}{L}\right] \tag{24}$$

$$[\phi_w]=\left[1-\frac{3x^2}{L^2}+\frac{2x^3}{L^3}\quad x-\frac{2x^2}{L}+\frac{x^3}{L^2}\quad \frac{3x^2}{L^2}-\frac{2x^3}{L^3}\quad -\frac{x^2}{L}+\frac{x^3}{L^2}\right] \tag{25}$$

The stiffness matrices (K_u, K_{uw}, K_w), the classical mass matrices (M_u^c, M_{uw}^c, M_w^c) and the nonlocal mass matrices (M_u^{nl}, M_{uw}^{nl}, M_w^{nl}) are obtained using Equations (23)-(25) as follows

$$K_u=\int_0^L A_1\left([\phi_u]'\right)^T[\phi_u]'\,dx \tag{26}$$

$$K_{uw} = -\left(\int_0^L B_1 \left([\phi_w]'' \right)^T [\phi_u]' \, dx + \int_0^L B_1 \left([\phi_u]' \right)^T [\phi_w]'' \, dx \right) \tag{27}$$

$$K_w = \int_0^L D_1 \left([\phi_w]'' \right)^T [\phi_w]'' \, dx \tag{28}$$

$$M_u^c = \int_0^L I_0 \left([\phi_u] \right)^T [\phi_u] dx \tag{29}$$

$$M_{uw}^c = -\left(\int_0^L I_1 \left([\phi_u] \right)^T [\phi_w]' \, dx + \int_0^L I_1 \left([\phi_w]' \right)^T [\phi_u] dx \right) \tag{30}$$

$$M_w^c = \int_0^L I_0 \left([\phi_w] \right)^T [\phi_w] dx + \int_0^L I_2 \left([\phi_w]' \right)^T [\phi_w]' dx \tag{31}$$

$$M_u^{nl} = (e_0 a)^2 \int_0^L I_0 \left([\phi_u]' \right)^T [\phi_u]' \, dx \tag{32}$$

$$M_{uw}^{nl} = -\left((e_0 a)^2 \int_0^L I_1 \left([\phi_u]' \right)^T [\phi_w]'' \, dx + (e_0 a)^2 \int_0^L I_1 \left([\phi_w]'' \right)^T [\phi_u]' dx \right) \tag{33}$$

$$M_w^{nl} = -(e_0 a)^2 \int_0^L I_0 \left([\phi_w] \right)^T \frac{\partial^2 [\phi_w]}{\partial x^2} dx + (e_0 a)^2 \int_0^L I_2 \left(\frac{\partial^2 [\phi_w]}{\partial x^2} \right)^T \frac{\partial^2 [\phi_w]}{\partial x^2} dx \tag{34}$$

The frequencies of FG nanobeam are found as follows

$$\left| K - \omega^2 M \right| = 0 \tag{35}$$

Here ω is frequency. *K* and *M* are total stiffness and mass matrices and given in Equations (36) and (37)

$$K = K_u + K_w + K_{uw} \tag{36}$$

$$M = M_u^c + M_{uw}^c + M_w^c + M_u^{nl} + M_{uw}^{nl} + M_w^{nl} \tag{37}$$

5. Numerical Results for Free Vibration of FG Nanobeam

In this section frequency values of SiC/SUS304 FG nanobeam are obtained with various dimensionless small-scale parameters (e_0a/L), power law exponents (k) and different boundary conditions such as S-S and C-C. The bottom surface of the beam is pure metal (SUS304) whereas the top surface of the beam is pure ceramic (SiC). Mechanical properties of nanobeam constituents are given in Table 1. Geometrical properties of the FG nanobeam are: b (width) = 100 nm, h (thickness) = 200 nm and L (length) = 10000 nm.

Table 1. Properties of FG nanobeams constituents [26]

	Properties	
	E (Gpa)	**ρ (kg/m^3)**
Silicon Carbide (SiC)	427	3210
Stainless Steel (SUS304)	207.78	8166

The frequency values obtained from the analyses of S-S FG nanobeam and C-C FG nanobeam with various e_0a/L ranging from 0 to 0.5 and various k ranging from 0 to 10 are presented in Table 2 and Table 3, respectively.

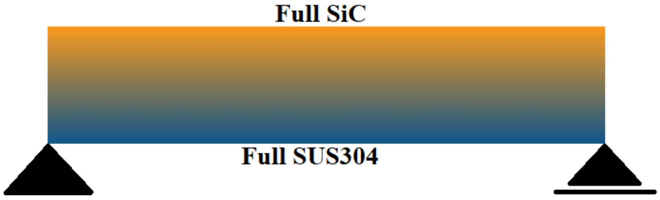

Fig. 3. Functionally graded S-S nanobeam

Table 2. Variation of first five frequencies (MHz) of FG nanobeam with k and e_0a/L (S-S)

k	**ω (MHz)**	**e₀a/L**					
		0	**0.1**	**0.2**	**0.3**	**0.4**	**0.5**
0	ω_1	10.4580	9.9772	8.8551	7.6106	6.5120	5.6163
	ω_2	41.8114	35.4031	26.0350	19.5949	15.4576	12.6820
	ω_3	93.9986	68.4054	44.0524	31.3427	24.1004	19.5126
	ω_4	166.9175	103.9357	61.7090	42.7962	32.5689	26.2355
	ω_5	260.4264	139.8566	78.9911	54.0604	40.9330	32.8930
0.2	ω_1	8.8233	8.4177	7.4710	6.4210	5.4941	4.7384
	ω_2	35.2750	29.8685	21.9649	16.5316	13.0411	10.6994
	ω_3	79.3007	57.7093	37.1643	26.4418	20.3320	16.4616
	ω_4	140.8103	87.6793	52.0573	36.1025	27.4749	22.1321
	ω_5	219.6787	117.9739	66.6317	45.6018	34.5284	27.7464
2	ω_1	6.1069	5.8262	5.1709	4.4442	3.8026	3.2796
	ω_2	24.4163	20.6741	15.2035	11.4427	9.0266	7.4058
	ω_3	54.8939	39.9478	25.7260	18.3037	14.0743	11.3951
	ω_4	97.4831	60.7005	36.0393	24.9938	19.0209	15.3221
	ω_5	152.1054	81.6851	46.1358	31.5747	23.9074	19.2116
5	ω_1	5.5038	5.2508	4.6602	4.0052	3.4271	2.9557

	ω_2	22.0051	18.6325	13.7021	10.3127	8.1352	6.6745
	ω_3	49.4742	36.0037	23.1861	16.4965	12.6848	10.2701
	ω_4	87.8615	54.7093	32.4822	22.5269	17.1435	13.8098
	ω_5	137.0985	73.6259	41.5840	28.4595	21.5487	17.3161
10	ω_1	5.1688	4.9312	4.3766	3.7615	3.2185	2.7758
	ω_2	20.6658	17.4984	12.8681	9.6850	7.6401	6.2682
	ω_3	46.4626	33.8121	21.7747	15.4924	11.9126	9.6449
	ω_4	82.5120	51.3783	30.5045	21.1554	16.0997	12.9690
	ω_5	128.7487	69.1418	39.0514	26.7262	20.2363	16.2615

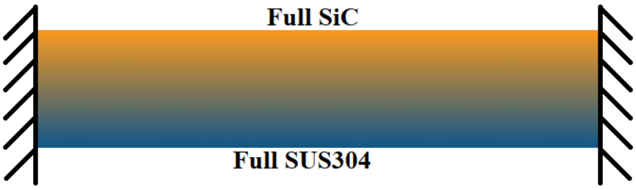

Fig. 4. Functionally graded C-C nanobeam

Table 3. Variation of first five frequencies (MHz) of FG nanobeam with *k* and e_0a/L (C-C)

k	**ω (MHz)**	**e0a/L**					
		0	**0.1**	**0.2**	**0.3**	**0.4**	**0.5**
0	ω_1	23.7062	22.3654	19.3760	16.2643	13.6693	11.6421
	ω_2	65.3103	53.9796	38.5572	28.5806	22.3751	18.2819
	ω_3	127.9220	90.6560	57.6512	41.0566	31.6753	25.7224
	ω_4	211.2074	128.1562	75.6097	52.4448	39.9337	32.1811
	ω_5	315.0270	165.2416	93.2586	64.0399	48.6300	39.1599
0.2	ω_1	20.0006	18.8694	16.3471	13.7218	11.5325	9.8221
	ω_2	55.1000	45.5403	32.5288	24.1120	18.8767	15.4234
	ω_3	107.9189	76.4787	48.6349	34.6354	26.7212	21.6993
	ω_4	178.1710	108.1072	63.7804	44.2395	33.6858	27.1461
	ω_5	265.7327	139.3795	78.6615	54.0159	41.0180	33.0302
2	ω_1	13.8432	13.0603	11.3147	9.4976	7.9823	6.7985
	ω_2	38.1389	31.5225	22.5165	16.6905	13.0666	10.6763
	ω_3	74.7053	52.9434	33.6689	23.9776	18.4989	15.0223
	ω_4	123.3507	74.8490	44.1601	30.6307	23.3236	18.7956
	ω_5	183.9983	96.5172	54.4729	37.4063	28.4054	22.8738
5	ω_1	12.4760	11.7704	10.1972	8.5597	7.1940	6.1271
	ω_2	34.3727	28.4098	20.2932	15.0425	11.7765	9.6222
	ω_3	67.3299	47.7170	30.3455	21.6109	16.6729	13.5395
	ω_4	111.1767	67.4631	39.8028	27.6084	21.0223	16.9411
	ω_5	165.8462	86.9977	49.1007	33.7173	25.6041	20.6181
10	ω_1	11.7167	11.0541	9.5766	8.0387	6.7562	5.7542
	ω_2	32.2807	26.6807	19.0580	14.1269	11.0597	9.0365
	ω_3	63.2313	44.8121	28.4980	20.2951	15.6578	12.7152
	ω_4	104.4073	63.3549	37.3788	25.9271	19.7421	15.9094
	ω_5	155.7450	81.6980	46.1094	31.6632	24.0442	19.3619

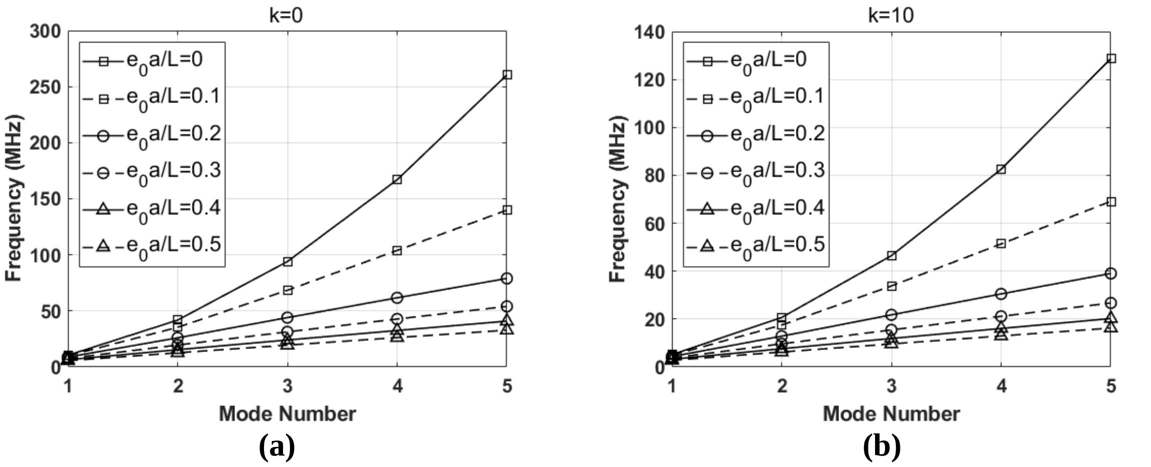

Fig. 5. The variation of the frequencies with mode numbers for different e_0a/L (S-S)
(a) $k=0$ (b) $k=10$

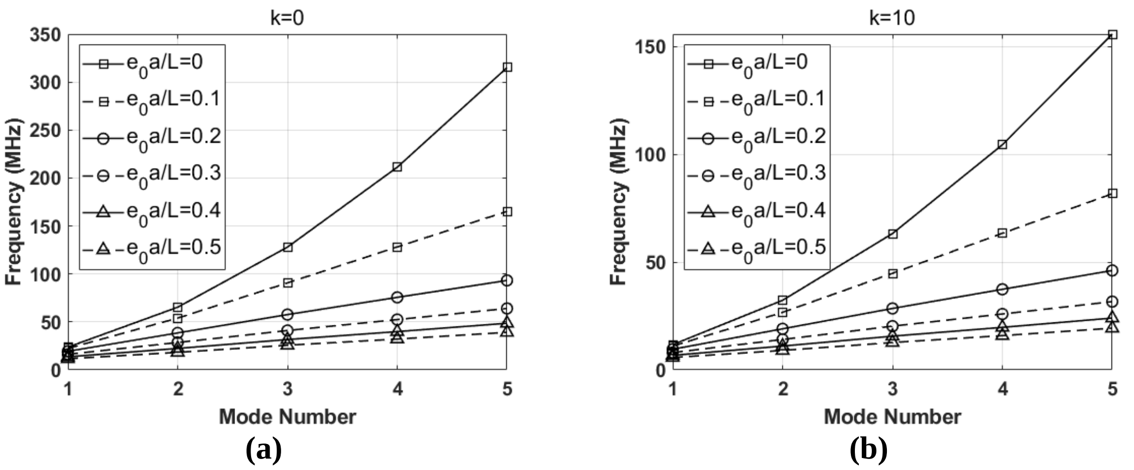

Fig. 6. The variation of the frequencies with mode numbers for different e_0a/L (C-C)
(a) $k=0$ (b) $k=10$

The effects of mode number on the frequency are respectively shown in Fig. 5 and Fig. 6. The frequency values of FG nanobeam increase as the mode number increase.

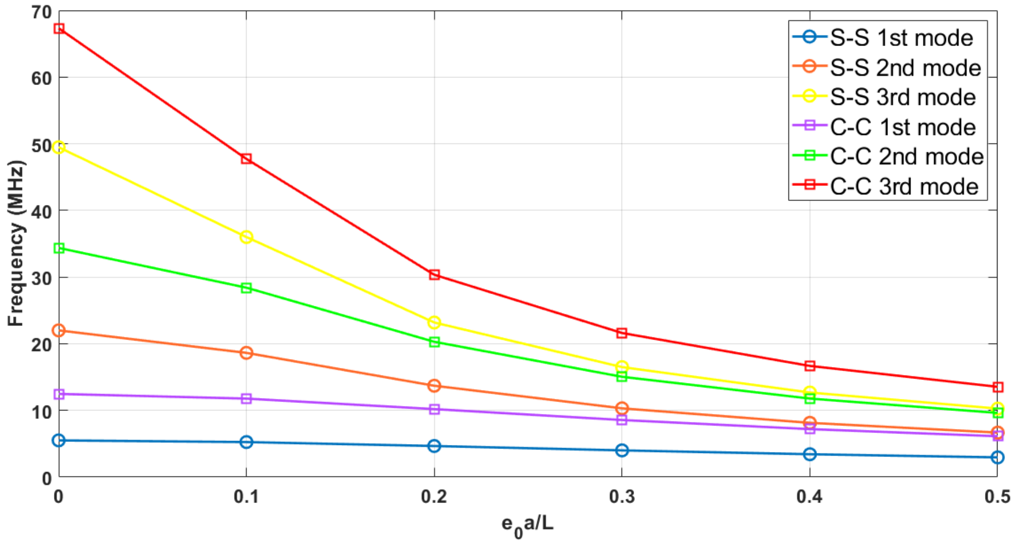

Fig. 7. The variation of the frequencies with e_0a/L ($k=5$)

The effects of e_0a/L (small-scale parameters) on the frequency are depicted in Fig. 7. The frequency values of FG nanobeam decrease as e_0a/L increases.

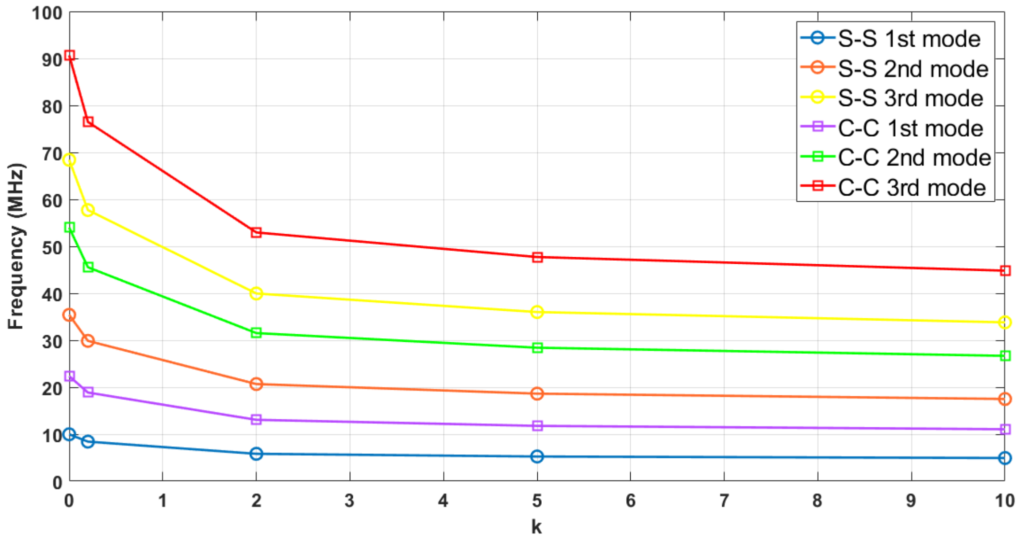

Fig. 8. The variation of the frequencies with k ($e_0a/L=0.1$)

The effects of k (power law exponent) on the frequency are depicted in Fig. 8. The frequency values of FG nanobeam decrease as k increases. Also it is clearly observed from the tables and figures that the frequency values of C-C boundary condition higher than the frequency values of S-S boundary condition.

6. Conclusions

Due to the small-scale effect, the properties and behaviours of nano structures are different from macro structures. In this paper, free vibration analysis of FG nanobeam composed of SiC and SUS304 is investigated based on the nonlocal elasticity theory and Euler-Bernoulli beam theory. Finite element method is a powerful numerical method. A nonlocal finite element formulation is developed for free vibration analysis of FG nanobeams, in this study. Solutions are obtained for S-S and C-C FG nanobeams. According to the obtained results

- By increasing e_0a/L, the frequency values decrease.
- Frequencies decrease with increasing k value.
- The frequency values of S-S smaller than the frequency values of C-C.
- The frequency values increase as the mode number increase.
- As the k increases, the properties of the FG nanobeam transform from ceramic to metal.

References

[1] Akgöz, B. and Civalek, Ö., Free vibration analysis of axially functionally graded tapered Bernoulli–Euler microbeams based on the modified couple stress theory. *Composite Structures,* 98, 314-322, 2013.

[2] Ebrahimi, F., Ghadiri, M., Salari, E., Hoseini, S.A.H. and Shaghaghi, G.R., Application of the differential transformation method for nonlocal vibration analysis of functionally graded nanobeams. *Journal of Mechanical Science and Technology*, 29(3), 1207-1215, 2015.

[3] Yayli, M.Ö. Torsional vibrations of restrained nanotubes using modified couple stress theory. *Microsystem Technologies*, 1-11, 2018.

[4] Ansari, R., Gholami, R., and Sahmani, S., Free vibration analysis of size-dependent functionally graded microbeams based on the strain gradient Timoshenko beam theory. *Composite Structures*, *94*(1), 221-228, 2011.

[5] Akgöz, B., and Civalek, Ö., Effects of thermal and shear deformation on vibration response of functionally graded thick composite microbeams. *Composites Part B: Engineering*, *129*, 77-87, 2017.

[6] Eringen, A.C., On differential equations of nonlocal elasticity and solutions of screw dislocation and surface waves. Journal of applied physics, 54(9), 4703-4710, 1983.

[7] Naghinejad, M. and Ovesy, H.R., Free vibration characteristics of nanoscaled beams based on nonlocal integral elasticity theory. *Journal of Vibration and Control*, 24(17), 3974-3988, 2018.

[8] Yaylı, M.Ö., Buckling Analysis of a Rotationally Restrained Single Walled Carbon Nanotube Embedded In An Elastic Medium Using Nonlocal Elasticity. *International Journal Of Engineering & Applied Sciences*, 8(2), 40-50, 2016.

[9] Eltaher, M.A., Emam, S.A. and Mahmoud, F.F., Static and stability analysis of nonlocal functionally graded nanobeams. *Composite Structures*, 96, 82-88, 2013.

[10] Thai, H.T., A nonlocal beam theory for bending, buckling, and vibration of nanobeams. *International Journal of Engineering Science*, 52, 56-64, 2012.

[11] Tounsi, A., Benguediab, S., Adda, B., Semmah, A. and Zidour, M., Nonlocal effects on thermal buckling properties of double-walled carbon nanotubes. *Advances in nano research*, 1(1), 1-11, 2013.

[12] Thai, S., Thai, H.T., Vo, T.P. and Patel, V.I., A simple shear deformation theory for nonlocal beams. *Composite Structures*, 183, 262-270, 2018.

[13] Ebrahimi, F. and Salari, E., Thermo-mechanical vibration analysis of nonlocal temperature-dependent FG nanobeams with various boundary conditions. *Composites Part B: Engineering,* 78, 272-290, 2015.

[14] Yayli, M.Ö., Buckling analysis of a cantilever single-walled carbon nanotube embedded in an elastic medium with an attached spring. *Micro & Nano Letters*, 12(4), 255-259, 2017.

[15] Yayli, M.Ö., On the axial vibration of carbon nanotubes with different boundary conditions. *Micro & Nano Letters*, 9(11), 807-811, 2014.

[16] Civalek, Ö., and Demir, C, Buckling and bending analyses of cantilever carbon nanotubes using the euler-bernoulli beam theory based on non-local continuum model. *Asian Journal of Civil Engineering*, 12(5), 651-661, 2011.

[17] Demir, Ç., and Civalek, Ö., A new nonlocal FEM via Hermitian cubic shape functions for thermal vibration of nano beams surrounded by an elastic matrix. *Composite Structures*, 168, 872-884, 2017.

[18] Naghinejad, M., and Ovesy, H.R., Viscoelastic free vibration behavior of nano-scaled beams via finite element nonlocal integral elasticity approach. *Journal of Vibration and Control*, 25(2), 445-459, 2019.

[19] Yayli, M.Ö., Effects of rotational restraints on the thermal buckling of carbon nanotube. *Micro & Nano Letters*, 14(2), 158-162, 2019.

[20] Mercan, K., Numanoglu, H.M., Akgöz, B., Demir, C. and Civalek, Ö., Higher-order continuum theories for buckling response of silicon carbide nanowires (SiCNWs) on elastic matrix. *Archive of Applied Mechanics*, 87(11), 1797-1814, 2017.

[21] Wang, C.M., Zhang, Y. Y., Ramesh, S.S. and Kitipornchai, S., Buckling analysis of micro-and nano-rods/tubes based on nonlocal Timoshenko beam theory. *Journal of Physics D: Applied Physics*, 39(17), 3904, 2006.

[22] Civalek, Ö. and Demir, Ç., Bending analysis of microtubules using nonlocal Euler–Bernoulli beam theory. *Applied Mathematical Modelling*, 35(5), 2053-2067, 2011.

[23] Kadıoğlu, H.G. and Yaylı, M.Ö., Buckling Analysis of Non-Local Timoshenko Beams by Using Fourier Series. *International Journal Of Engineering & Applied Sciences*, 9(4), 89-99, 2017.

[24] Zargaripoor, A., Daneshmehr, A., Isaac Hosseini, I., and Rajabpoor, A., Free vibration analysis of nanoplates made of functionally graded materials based on nonlocal elasticity theory using finite element method. *Journal of Computational Applied Mechanics*, 49(1), 86-101, 2018.

[25] Reddy, J.N., *Energy Principles and Variational Methods in Applied Mechanics,* John Wiley & Sons; 2nd edition, 2002.

[26] Talha, M. and Singh, B.N., Static response and free vibration analysis of FGM plates using higher order shear deformation theory. *Applied Mathematical Modelling*, 34(12), 3991-4011, 2010.